Int. J. Heat Mass Transfer. Vol. 36, No. 3, pp. 617–625, 1993
Printed in Great Britain

0017-9310/93 $6.00 + 0.00

Improved heat-transfer models for fibrous insulations

C. STARK and J. FRICKE†
Physikalisches Institut Universität, Am Hubland, D-8700 Würzburg, F.R.G.

(*Received* 30 *March* 1992)

Abstract—We have developed three improved heat transfer models, which allow prediction of the thermal conductivity of evacuated and gas-filled fibrous insulations. These models take into account the coupling between the solid conduction of the fibre system and the gaseous conduction of the gas in the pore space. They use cell configurations, in which the contact resistance between two neighbouring fibres can be modelled by statistical considerations. Results from the derived models are compared with data obtained for 15 different fibre insulations, which have been investigated in evacuable, load-controlled guarded hot plate systems. Experimentally changed parameters were gas pressure, temperature and density of specimens.

1. INTRODUCTION

MEASUREMENTS on fibrous insulations [1–7] show that in non-evacuated fibrous insulations the combined solid and gaseous thermal conductivity λ_{sg} is underestimated if the thermal conductivity of the gas λ_g and the thermal conductivity λ_s of the solid fibres are superimposed linearly (see Table 1). One finds $\lambda_{sg} > \lambda_s + \lambda_g$ for densities ρ higher than 5 kg m^{-3}. At $\rho = 300$ kg m^{-3} the excess is about 20%.

To account for this effect several heat transfer models were developed [2–4, 8]. However, there was a lack of sufficient agreement between results from these models and recent measurements on 16 different fibrous insulations in several evacuable guarded hot plate systems at the Physics Institute/University Würzburg as a function of air pressure, temperature and density. In the above models all fibres are either assumed to be perpendicular to the macroscopic heat flow or randomly oriented. Bhattacharyya [3] suggests a 50 : 50 split between these two extreme assumptions. The new improved heat transfer model based on Fricke [9] and Bhattacharyya [3], but takes into consideration a variable orientation of the fibres and adjustable contacts between the fibres [7]. The mean orientation varies with density and external pressure and/or is assigned by production.

2. THEORETICAL MODELS

The heat flux passing through a fibrous insulation is represented by the following equation:

$$q = q_{sg} + q_r. \tag{1}$$

Using Fourier's empirical law $q = -\lambda \operatorname{grad} T$ and assuming that grad T is the same for all types of heat transfer, one gets for the total thermal conductivity

$$\lambda_{total} = \lambda_{sg} + \lambda_r. \tag{2}$$

In fibrous insulations with densities greater than 20 kg m^{-3} no convection occurs because the fibres subdivide the gas into sufficiently small pores [3]. Radiative transfer in such insulations with layers of several cm can be considered a local phenomenon. Thus the additive superposition of λ_{sg} and λ_r in equation (2), valid for optically thick insulations, is justified. λ_r can be determined either calorically or from infrared optical measurements [10].

As stated above, the combined solid and gaseous conductivity λ_{sg} generally is larger than the sum of $\lambda_s + \lambda_g$.

The derivation of λ_{sg} is pursued using a three-step approach, in which firstly a basic model then a modified model and finally a model with suitable connection parameters are considered.

2.1. *Basic model (BM)*

In this model specimens with any mean orientation can be calculated by use of a parameter Z, which represents the fraction of all fibres oriented perpendicularly to the macroscopic heat flow. Bhattacharyya's extreme orientations yield $Z = 1$ (all fibres perpendicular to heat flow) and $Z = 0.66$ (random orientation of fibres). Each specimen is associated with a mean orientation and a corresponding Z.

Table 1. Typical thermal conductivities of non-evacuated fibrous insulations at $T = 300$ K. λ_g (300 K) $= 26 \times 10^{-3}$ W m^{-1} K^{-1}

	ρ (kg m^{-3})				
	5	20	50	100	300
λ_r in 10^{-3} W m^{-1} K^{-1}	50	15	4	3	1
λ_s in 10^{-3} W m^{-1} K^{-1}	0	0	1	2	4
λ_{sg} in 10^{-3} W m^{-1} K^{-1}	26	29	30	32	37

† Author to whom correspondence should be addressed.

NOMENCLATURE

a_{ct}	contact radius
A	connection parameter
A_{ct}	area of one contact
c_L	velocity of light in vacuum
Cr	ratio of thermal conductivity of gas to thermal conductivity of solid material, λ_g/λ_s
d	thickness of the specimen
D	pore diameter of the fibrous insulation
e_R^*	Rosseland mean value of the specific extinction
$f_R(\Lambda \cdot T)$	Rosseland function
G	fit parameter
h	Planck's constant
$h(t)$	probability function for fibre orientations
k_B	Boltzmann's constant
l	length of fibre (diagonal of the cell)
l_m	mean free path
m	height of the fibre–gas cell in units of the fibre diameter
m''	mass per area
n	refractive index of the specimen
n_0	refractive index of the solid material
$o+1$	area of a fibre–gas cell in units of the contact area
p_g	gas pressure
p_{ext}	external pressure
q	heat flux
r	radius of a fibre
R_g	thermal resistance by gas
R_{ct}	thermal resistance of a contact
R_{MM}	thermal resistance of a fibre–gas cell
S_{cell}	area of a fibre–gas cell
T	temperature [K]
T_h, T_c	temperature of the hot and cold plate
T_r	mean radiative temperature, $T_r^2 = 1/4 \cdot (T_h^2 + T_k^2) \cdot (T_h + T_k)$
Vr	ratio of the volume of fibre and gas, $\rho/(\rho_0 - \rho)$
Y_0	Young's modulus
Z	part of all fibres, which are orientated perpendicularly to the macroscopic heat flow.

Greek symbols

β_K	constant (1.554 for nitrogen) (different for different gases)
ε	emissivity of the plates
ϑ, φ	angles, which describe the orientation of the fibre in the cell
ϑ_0, φ_0	mean orientational fibre angles
λ	thermal conductivity
λ_e	thermal conductivity of evacuated specimen
λ_g	thermal conductivity by gas (nitrogen)
λ_{ne}	thermal conductivity of gas-filled, non-evacuated specimen
λ_r	thermal conductivity by radiation
λ_s	thermal conductivity by solid fibres
λ_{sg}	thermal conductivity by solid fibres, gas and their coupling
λ_0	thermal conductivity of the solid material
Λ	wavelength
μ_0	Poisson's number of the fibre material
ρ	density of the specimen
ρ_0	density of the fibre material
σ	Stefan–Boltzmann constant.

It is supposed that the heat transfer in fibrous insulations with any mean orientation of the fibres can be composed of a fibre fraction with an orientation perpendicular to the macroscopic heat flow and a parallel fraction. As in Bhattacharyya's model, the following are assumed:

(i) The fibrous insulation can be approximated as a homogeneous medium of thermal conductivity λ_{sg}.

(ii) Interactions between fibres influencing λ_{sg} can be averaged over a unit volume, a cell.

(iii) Any individual fibre can be assumed to be a spheroid whose major axis is very large compared with the minor axis.

With these assumptions the thermal conductivity λ_{sg} of solid fibres, gas and their coupling can be derived:

$$\lambda_{sg}^{BM} = \lambda_0 \cdot \left(1 + \frac{Cr-1}{1+Vr(1+Z\cdot(Cr-1)/(Cr+1))}\right). \quad (3)$$

$Cr = 0$ corresponds to evacuated specimens, for which the solid thermal conductivity λ_s is

$$\lambda_s^{BM} = \lambda_0 \cdot Vr \cdot (1-Z)/(1+Vr\cdot(1-Z)). \quad (4)$$

2.2. *Modified model (MM)*

It proved necessary to pay attention to the contacts between fibres, which act as thermal resistances. The thermal conductivity of the solid phase, the gas and the coupling effects for the MM can be calculated using the thermal resistances in Fig. 1.

Furthermore, the following assumptions are made (Fig. 2): while in the BM the cell height is $m \cdot 2r$, in the MM it is $(m+1) \cdot 2r$. The contact area is A_{ct}, the effective area of the gas volume acting as a parallel resistance R_s is $o \cdot A_{ct}$.

The contact resistance R_{ct} is calculated according to Kaganer [1], using the contact radius of Hertz [11] for elastic deformations of cylinders with $a_{ct} \ll r$

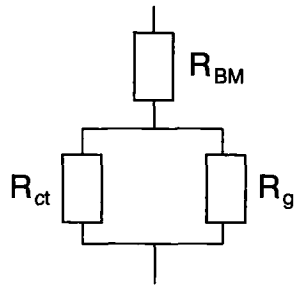

FIG. 1. Circuit diagram of the thermal resistances (R) of basic model (BM), contact (ct) and gas (g).

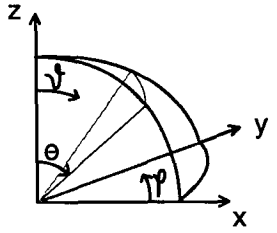

FIG. 3. All fibres with an orientation angle $\vartheta < \Theta$ are considered parallel to the macroscopic heat flow, all those with $\vartheta > \Theta$ perpendicular.

$$R_{ct} = 1/(2a_{ct}\lambda_{sol}). \tag{5}$$

Thus the cell area is $S_{cell} = (o+1)A_{ct}$.

$$\lambda_{ss}^{MM} = \frac{(m+1)\cdot 2r}{S_{cell}\left(R_{BM} + \left(\frac{1}{R_g} + \frac{1}{R_{ct}}\right)^{-1}\right)}. \tag{6}$$

Figure 3 defines the angles which describe the orientation of a fibre. Because of rotation symmetry relative to the macroscopic heat flow (z-axis) and the symmetry relative to the x,y-plane it is sufficient to consider only one-eighth of the total solid angle to calculate the mean fibre orientation and the corresponding Z.

To calculate the size parameters m and o of the cell two functions for the orientational probability of the fibres can be used:

- A step function

$$h(\vartheta) = \begin{cases} \kappa & \vartheta < \Theta \\ \xi\cdot\kappa & \vartheta \geqslant \Theta \end{cases} \qquad \xi = \frac{1}{2/Z-2} \tag{7}$$

($\xi = 1$ for randomly oriented fibres).

- A continuous function

$$h(\vartheta) = \begin{cases} \beta\cdot\vartheta & \vartheta < \Theta \\ (\beta\cdot\Theta - \gamma\cdot\Theta) + \gamma\cdot\vartheta & \vartheta \geqslant \Theta \end{cases} \tag{8}$$

with $\beta > 0$

$$\frac{\beta}{\gamma} = \frac{(1-Z)\cdot(1-\sin\Theta)}{Z\cdot\sin\Theta - \Theta\cdot\cos\Theta}.$$

For $\beta \ll \gamma$ this function is a good description for specimens with fibres orientated nearly perfectly perpendicular to the macroscopic heat flow.

With these functions the fraction of fibres which are perpendicular to the macroscopic heat flow can be calculated

$$Z = \frac{\int_0^{90°}\int_\Theta^{90°} h(\vartheta) l^2 \sin\vartheta \,\mathrm{d}\vartheta \,\mathrm{d}\varphi}{\int_0^{90°}\int_0^{90°} h(\vartheta) l^2 \sin\vartheta \,\mathrm{d}\vartheta \,\mathrm{d}\varphi}. \tag{9}$$

Θ is the critical angle which separates the fibres which are considered parallel and perpendicular to the macroscopic heat flow, respectively (Fig. 3). Knowing that for randomly orientated fibres $h(\vartheta) = \text{const.}$ and $Z = 0.66$, the angle Θ, used for both functions, can be derived from equation (9)

$$\cos\Theta = 2/3, \quad \Theta = \arccos 2/3. \tag{10}$$

For both probability functions the mean angle ϑ_0 (Fig. 4) and φ_0 can be calculated as a function of Z. φ_0 is 45°, irrespective of Z.

m and o are given as a function of the fibre orientation and therefore of Z:

$$m+1 = \frac{1}{2}\frac{l}{r}\cos\vartheta_0 \tag{11}$$

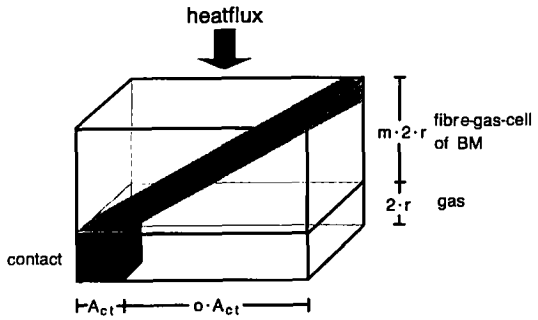

FIG. 2. Cell of the modified model.

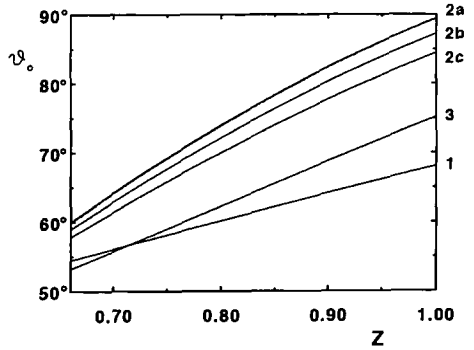

FIG. 4. Mean orientation angle ϑ_0 as a function of Z for both probability functions (equations (7) and (8)).

Table 2. Density ρ_0, index of refraction n_0, Young's modulus Y_0 and Poisson's number μ_0 of the fibre material [13, 14]

Material	ρ_0 (kg m^{-3})	n_0	Y_0 (N m^{-2})	μ_0
b.board, b.wool	2520	1.5	10^{11}	0.25
b.paper	2200	1.5	10^{11}	0.25
SF 1, SF 2	2700	1.5	10^{11}	0.25
b.1, b.2	2500	1.5	10^{11}	0.25
SiO_2 A, B, C, D	2200	1.4	10^{11}	0.25
P A, P B1, P B2	1380	1.5	32×10^8	0.35

$$o+1=\left(\frac{l}{r}\right)^{2/3}\frac{(0.5\sin\vartheta_0)^{1/3}}{\pi(1.5(1-\mu_0^2)p_{ext}/Y_0)^{2/3}} \quad (12)$$

$$\frac{l}{r}=\left(\frac{\pi\rho_0/\rho}{0.5\sin^2\vartheta_0\cos\vartheta_0}\right)^{1/2}. \quad (13)$$

2.3. *Modified model with connection parameter (MMC)*

In a real fibrous insulation not all adjacent fibres are in direct contact with each other. We thus define a unit cell of the same size as in the MM. This cell is divided into eight subunits, each having the structure of one-eighth of a MM cell. In the centre of the unit cell the eight corners of the subunits touch one another. The directions of the fibres in these subunits can be chosen in 4^8 possible ways. The heat flux may be characterized by the maximal or minimal number of fibres, which connect the centre with the cold or, respectively, the hot side of the unit cell. These two limiting cases yield the maximal and minimal value of the connection parameter A: 0.6836 and 0.5384, respectively. For the following calculations the arithmetic mean value $A = 0.611$ is used.

The combined gaseous and solid thermal conductivity according to the MMC is

$$\lambda_{sg}^{MMC}=(m+1)\left\{\frac{m}{\lambda_{sg}^{BM}}+\frac{o+1}{o}\frac{1}{\lambda_g+\dfrac{4\lambda_0 Ar}{o\pi a_{ct}}}\right\}^{-1} \quad (14)$$

λ_{sg}^{BM} is given by equation (3).

In the three improved heat transfer models the quantity Z is a free parameter. In some cases Z was available from the product information provided by the producer.

3. MEASUREMENTS

To calculate the radiative thermal conductivity λ_r IR-optical measurements are performed with a commercial FTIR-spectrometer in the wavelength region 2.5–45 μm. The effective spectral mass-specific extinction coefficient $e^*(\Lambda)$ is derived from reflection and transmision measurements using an integrating sphere. The effective specific extinction coefficient $e_R^*(T)$ as a function of temperature can be calculated using the Rosseland distribution function $f_R(\Lambda, T)$ [12]

Table 4. Thermal conductivity $\lambda_0(T)$ of used solid materials [14, 15]

Material	Temperature range (K)	λ_0 (W m^{-1} K^{-1})
basalt	250–500	$0.4898+1.989\times10^{-3}\,(T/\mathrm{K})$
b.glass	250–500	$0.6809+1.377\times10^{-3}\,(T/\mathrm{K})$
	250–650	$0.5907+1.871\times10^{-3}\,(T/\mathrm{K})$ $-6.299\times10^{-7}\,(T^2/\mathrm{K}^2)$
SiO_2	250–700	$0.9670+1.336\times10^{-3}\,(T/\mathrm{K})$
	350–900	$0.2406+7.047\times10^{-3}\,(T/\mathrm{K})$ $-1.502\times10^{-5}\,(T^2/\mathrm{K}^2)$ $+1.520\times10^{-8}\,(T^3/\mathrm{K}^3)$ $-4.597\times10^{-12}\,(T^4/\mathrm{K}^4)$
polyester	290	0.26

Table 3. Density ρ, thickness d, mass per area m'' and index of refraction n of fibrous insulations in hot plate systems with external load p_{ext} and boundary emissivity ε

Material	ρ (kg m^{-3})	d (10^{-3} m)	m'' (kg m^{-2})	n^2	p_{ext} (10^3 Pa)	ε
b.board	300	18.6	5.77	1.109	93.2	0.77
b.wool	314	11.0	3.46	1.114	$\leqslant$93.2	0.77
b.paper nt	321	8.0	2.57	1.135	310.9	0.77
b.paper t	425	6.1	2.57	1.181	310.9	0.77
SF 1	105	25.5	2.67	1.037	$\leqslant$8.0	0.80
SF 2	42	25.7	1.09	1.014	$\leqslant$0.40	0.80
b.1	43	25.7	1.10	1.015	$\leqslant$0.27	0.80
b.2	76	25.7	1.96	1.027	$\leqslant$3.6	0.80
SiO_2 A	80	5.4	0.426	1.027	10.0	0.77
SiO_2 B	80	9.4	0.751	1.027	10.0	0.77
SiO_2 C	80	10.0	0.800	1.027	10.0	0.77
SiO_2 D	160	5.0	0.800	1.054	100.0	0.77
P A	21	12.8	0.269	1.013	5.0	0.80
P B1	54	8.0	0.45	1.035	$\leqslant$25.0	0.99
P B2	155	8.0	1.35	1.102	$\leqslant$120.0	0.99

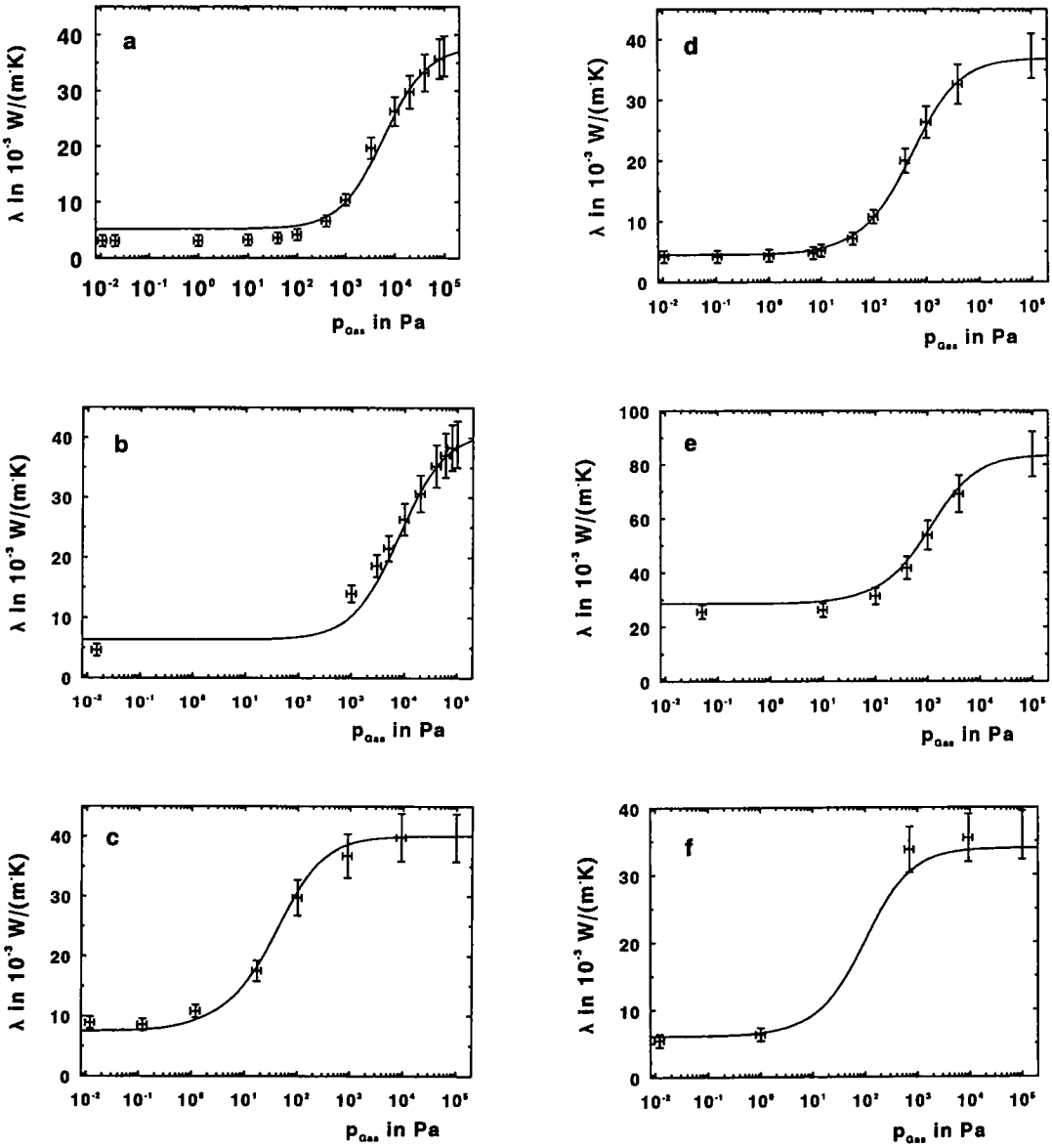

FIG. 5. Thermal conductivity as a function of air pressure p_g. +, measurements, error bars are also given; solid line, MMC calculation using the parameters D and Z [7]: (a) non-tempered b.paper; $T = 324$ K, $\rho = 321$ kg m^{-3}, $D = 3.5$ μm and $Z = 0.93$; (b) tempered b.paper; $T = 324$ K, $\rho = 425$ kg m^{-3}, $D = 2.5$ μm and $Z = 0.90$; (c) SF 1; $T = 328$ K, $\rho = 105$ kg m^{-3}, $D = 500$ μm and $Z = 0.82$; (d) SiO_2 C; $T = 339$ K, $\rho = 80$ kg m^{-3}, $D = 40$ μm and $Z = 0.90$; (e) SiO_2 C; $T = 698$ K, $\rho = 80$ kg m^{-3}, $D = 40$ μm and $Z = 0.90$; (f) P B1; $T = 303$ K, $\rho = 54$ kg m^{-3}, $D = 200$ μm and $Z = 0.66$.

$$\frac{1}{e^*_R(T)} = \int_0^\infty \frac{1}{e^*(\Lambda)} f_R(\Lambda T)\, d\Lambda \qquad (15)$$

with

$$f_R(\Lambda T) = \frac{15}{4\pi^4}\left[\frac{c_L h}{\Lambda k_B T}\right]^5 \frac{1}{\Lambda} \frac{\exp\{hc_L/(k_B \Lambda T)\}}{[\exp\{hc_L/(k_B \Lambda T)\} - 1]^2}. \qquad (16)$$

The caloric measurements were carried out in several evacuable, load-controlled guarded hot plate systems at our institute. These systems can be evacuated down to 10^{-2} Pa and operated between temperatures of 270 and 840 K.

The fibres of the investigated specimens consist of borosilicate glass (b.), basalt (SF), SiO_2 or polyester (P). Table 2 shows the material data and Table 3 the specimen data. If pegs are used to define a certain distance between the plates, the external pressure in Table 3 is an upper limit and is marked by '$\leqslant$'. The

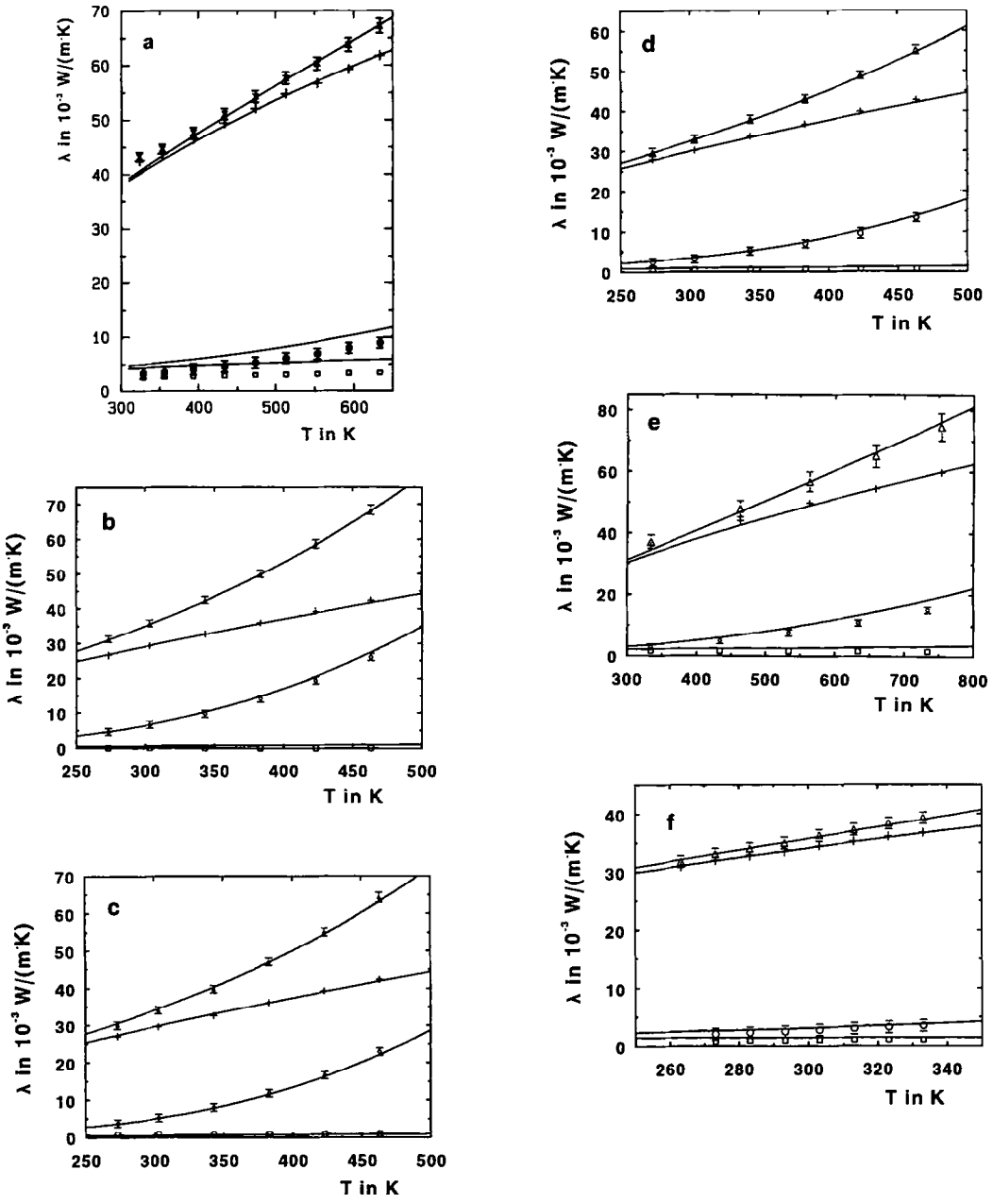

FIG. 6. Thermal conductivity as a function of temperature. Measurements: △, λ_{nc}; +, λ_{sg}; ○, λ_e; □, λ_s; solid line, MMC calculation using Z and D as follows [7]: (a) tempered b.wool; $Z = 0.85$ and $D = 5\ \mu m$; (b) SF 2; $Z = 0.82$; (c) b.1; $Z = 0.80$; (d) b.2; $Z = 0.88$; (e) SiO_2 D; $Z = 0.97$; (f) P B2; $Z = 0.66$.

solid conductivity λ_0 of the fibre materials is given in Table 4.

4. COMPARISON OF CALORIC MEASUREMENTS AND MMC

In order to compare the measurements of the thermal conductivity λ_{sg}^{exp} and λ_s^{exp} of evacuated and gas-filled specimens, respectively, with the results from the MMC the following conversions were made:

(a) To get rid of the radiative contributions, the measured extinction coefficients $e_R^*(T)$ were converted into radiative conductivities [10]

$$\lambda_r = T_r^3 \frac{4\sigma n^2 d}{\left(\frac{2}{\varepsilon} - 1\right) + \frac{3m''}{4} e_R^*(T)}. \qquad (17)$$

λ_r was then subtracted from the conductivity λ_e^{exp} for the evacuated specimens, or from λ_{nc}^{exp} for the non-evacuated specimens to yield λ_s^{exp} and λ_{sg}^{exp}, respectively.

(b) λ_e^{MMC}, calculated from the MMC, contains the thermal conductivity by radiation (equation (17)) and the solid conductivity λ_s^{MMC} of the fibrous system; the latter is derived by using $\lambda_g = 0$ in equations (14) and (3). For $Z > 0.66$ the continuous function is used. For $Z = 0.66$ the step function best describes the fibre orientation.

(c) Similarly, $\lambda_{ne}^{MMC} = \lambda_r + \lambda_{sg}^{MMC}$ is calculated with $\lambda_g = \lambda_{nitrogen}$.

4.1. *Comparison of MMC and thermal conductivity measurements as a function of air pressure*

For each material listed in Table 3 measurements at constant temperature and fixed temperature difference between the cold and the hot plate were performed. For SiO_2 the measurements were conducted at $T_r = 339$ and 698 K. The theoretical values are calculated by using the thermal conductivity of gas as a function of air pressure, temperature and mean pore diameter

$$\lambda_g = \frac{\lambda_{g0}}{(1+2\beta_K l_m/D)} \tag{18}$$

with

$$l_m = \frac{k_B T}{2^{1/2} p_g \sigma_0}. \tag{19}$$

λ_{g0} is the gaseous conductivity of a free gas (mean free path l_m large compared to pore width D).

The two free parameters are the fibre orientation Z and the pore diameter D, which allow the theory to be fitted to the measurements. For some specimens (Figs. 5(a) and (b)) not the thermal conductivity λ_{g0} of a free gas is not reached, even for $p_g = 10^5$ Pa. In general, excellent agreement is obtained between experimental and theoretical values (Fig. 5).

4.2. *Comparison of MMC and thermal conductivity data as a function of temperature*

For each material the thermal conductivity as a function of temperature is measured in the largest possible temperature range, both for $p_g = \text{const.} < 10^{-1}$ Pa and for $p_g = \text{const.} \approx 10^5$ Pa (Fig. 6).

For materials, for which $\lambda_g < \lambda_{g0}$ even at $p_{gas} = 10^5$ Pa, the gaseous thermal conductivity $\lambda_g(T)$ is calculated using the pore diameter fitted with equation (18). Furthermore, equations (14) and (3) are used (Fig. 6(a)). The free parameter Z is fitted to give the best agreement for all four conductivities λ_s, λ_e, λ_{sg} and λ_{ne}. For SF 1, b.1 and b.2 the fibre orientation was provided by the producer. The polyester fibres had a fixed fibre orientation of $Z = 0.66$. Using these Z values good agreement between measurements and theory is obtained.

4.3. *Comparison of MMC and thermal conductivity measurements as a function of density*

For the two specimens P B2 and b.1 the density was varied.

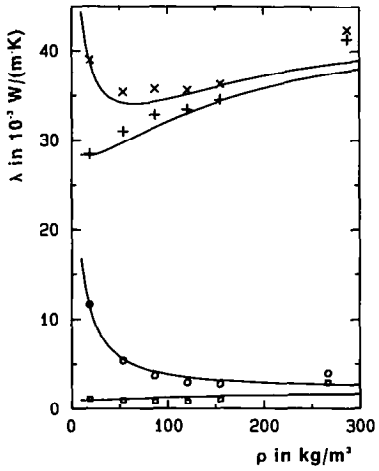

FIG. 7. Thermal conductivity as a function of density for P B2 at $T = 303$ K. Measurements: ×, λ_{ne}; +, λ_{sg}; ○, λ_e; □, λ_s; solid line, MMC calculation with $Z = 0.66$.

In b.1 the fibres are not connected, therefore they tend to orientate perpendicularly to the macroscopic heat flow under external pressure p_{ext}. Also, the contact area increases with increasing external pressure. The measurements could be fitted best by using

$$\begin{aligned} Z = {} & 0.64 + 5.80\times10^{-3}\,\rho\ (\text{kg m}^{-3}) \\ & -5.57\times10^{-5}\,(\rho\ (\text{kg m}^{-3}))^2 \\ & +2.42\times10^{-7}\,(\rho\ (\text{kg m}^{-3}))^3 \\ & -3.93\times10^{10}\,(\rho\ (\text{kg m}^{-3}))^4 \end{aligned}$$

and $p_{ext} = 0.4\ (\rho\ (\text{kg m}^{-3}) - 27.5)^{2.3}$ Pa (Fig. 7).

P B2 fibres form a network with bonded fibre crossings. Here the mean fibre orientation and the contact areas do not change under compression (Fig. 8).

4.4. *Comparison of MMC with other models*

The comparison is made for evacuated and gas-filled samples.

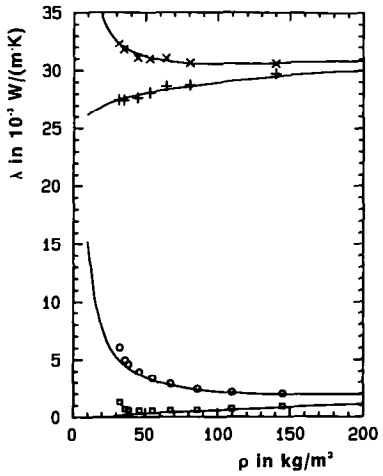

FIG. 8. Thermal conductivity as a function of density for b.1 at $T = 283$ K. Measurements: ×, λ_{ne}; +, λ_{sg}; ○, λ_e; □, λ_s; solid line, MMC calculation with equation (21).

(I) Additive superpositions of the three heat transfer components, radiation, solid conduction and gas conduction

$$\lambda_e = \lambda_{sg}(\lambda_g = 0) + \lambda_r \quad \text{and} \quad \lambda_{nc} = \lambda_c + \lambda_g.$$

(II) Model of Bhattacharyya [3] and Hasselmann [8] for all fibres perpendicular to the macroscopic heat flow.

(III) Model of Bhattacharyya [3] and McKay [4] for the specimens having fibres with random orientation.

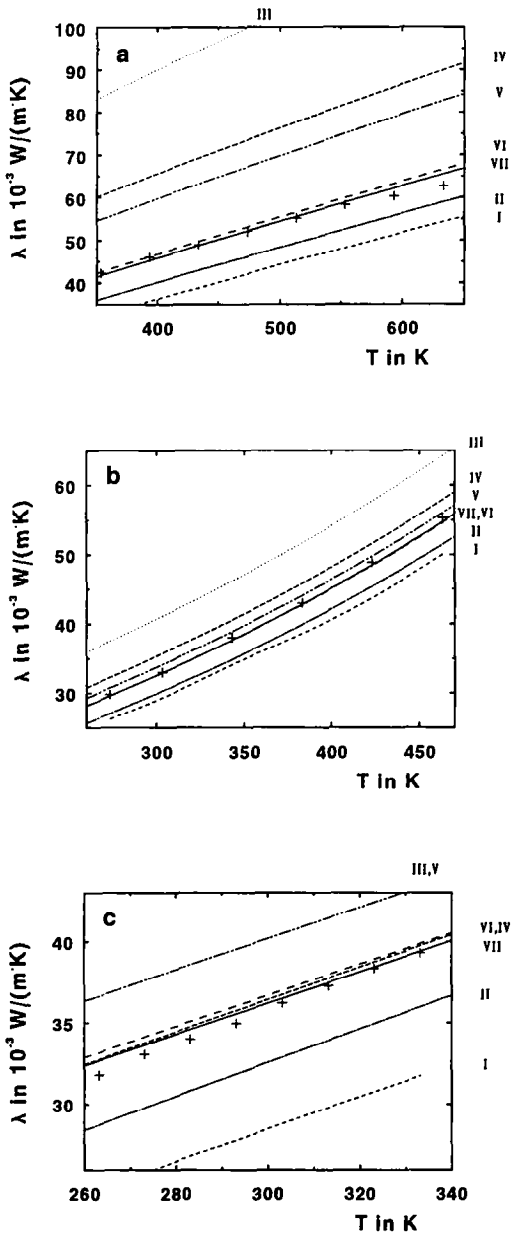

FIG. 9. Comparison of the thermal conductivities of gas-filled specimens: measurements (+) and models II–VII. For models V–VII we used the following Z: (a) b.board with $\rho = 300$ kg m^{-3}; $Z = 0.87$; (b) b.2 with $\rho = 76$ kg m^{-3}; $Z = 0.88$; (c) P B2 with $\rho = 155$ kg m^{-3}; $Z = 0.66$.

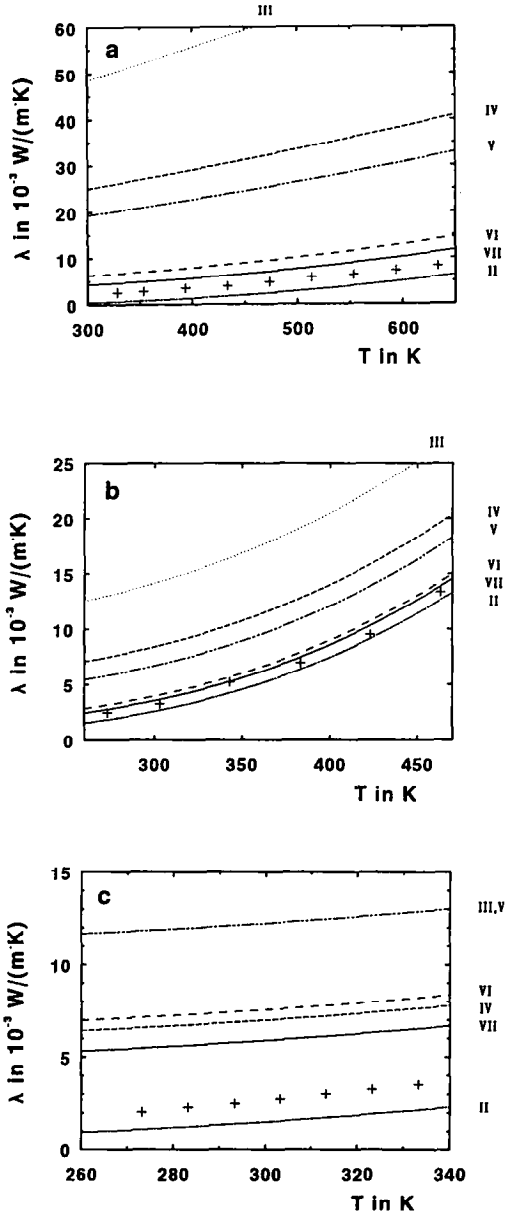

FIG. 10. Comparison of the thermal conductivities of evacuated specimens: measurements (+) and models II–VII. For models V–VII we used the following Z: (a) b.board with $\rho = 300$ kg m^{-3}; $Z = 0.87$; (b) b.2 with $\rho = 76$ kg m^{-3}; $Z = 0.88$; (c) P B2 with $\rho = 155$ kg m^{-3}; $Z = 0.66$.

(IV) Model of Bhattacharyya [3] for building insulations, a 50 : 50 split between the values of model II and model III.

(V) Basic model (BM).

(VI) Modified model (MM).

(VII) Modified model with connection parameter (MMC).

Models II to IV are special cases of model V, they work with fixed fibre orientations $Z = 1$, 0.66 and

0.83, respectively. The comparison was performed for three selected specimens, which differ in fibre material, useful temperature range and density. With models II–VII λ_{sg} is calculated; λ_r is added to get the total conductivities λ_e and λ_{ne} in the evacuated and non-evacuated state. Model II always gives $\lambda_s = 0$, if $\lambda_g = 0$ and therefore λ_e (model II) $= \lambda_r$. A suitable model for calculation of λ_s exists only for $Z = 1$ [1]. Hence a comparison of evacuated data with model I is not very helpful. Figure 9 shows the thermal conductivity of gas-filled specimens as a function of temperature for b.board, b.2 and P B2. Figure 10 displays the conductivities of the same materials under evacuation.

5. DISCUSSION

Figure 9 shows that models I and II always predict a thermal conductivity, which is too low. Values from model III are too high and model IV works only for some special specimens. Models II–IV are not suitable to account for the variety of fibre orientations. The agreement between measurements and the three improved models is good; best results are obtained with MMC (model VII). The fibre orientations of b.1 and b.2 reported by the producer lead to acceptable or very good agreement with measured values.

Figure 10 shows the thermal conductivity of evacuated specimens. Models II and III yield too low and too high values, respectively. The solid thermal conductivity λ_s calculated by models III–VII is too high and therefore the same holds for $\lambda_e = \lambda_s + \lambda_r$.

The results of model VII, especially λ_s, are influenced by the pressure on the contacts and the connection parameter A.

Overall, the results from model VII agree best with measurements, both for evacuated and for gas-filled fibrous insulations as a function of air pressure, temperature and density.

REFERENCES

1. M. G. Kaganer, Thermal insulation in cryogenic engineering, Israel Program for Scientific Translations, Jerusalem (1969).
2. C. Bankvall, Heat transfer in fibrous materials, *J. Testing Evaluation* **1**, 235–243 (1973).
3. R. K. Bhattacharyya, Heat-transfer model for fibrous insulations, thermal insulation performance, *ASTM STP* **718** (Edited by D. L. McElroy and R. P. Tye), pp. 272–286. American Society for Testing and Materials (1980).
4. N. L. McKay, T. Timusk and B. Farnworth, Determination of optical properties of fibrous thermal insulation, *J. Appl. Phys.* **55**, 4064–4071 (1984).
5. J. Hetfleisch, Wärmetransport in Glasfaser-Isolationen bei hohen Temperaturen, Diplome Thesis, Phys. Inst., University of Würzburg, Report E21-1288-2 (1988).
6. J. Kuhn, Wärmetransport in konventionellen Faser- und Schaumdämmstoffen, Diplome Thesis, Phys. Inst., University of Würzburg, Report E21-0589-3 (1989).
7. C. Stark, Wärmetransport in Faserisolationen: Kopplung zwischen Festkörper- und Gaswärmeleitung, Ph.D. Thesis, Phys. Inst., University of Würzburg, Report E21-0691-4 (1991).
8. D. P. H. Hasselman and L. F. Johnson, Effective thermal conductivity of composites with interfacial thermal barrier resistance, *J. Composite Mat.* **21**, 508–515 (1987).
9. H. Fricke, A mathematical treatment of the electric conductivity and capacity of disperse systems, *Phys. Rev.* **24**, 575–587 (1924).
10. J. Fricke and R. Caps, Heat transfer in thermal insulations, recent progress in analysis, *Int. J. Thermophys.* **9**, 885–895 (1988).
11. H. Hertz, Über die Berührung fester elastischer Körper, *J. Reine Angew. Math.* **29**, 156–171 (1882).
12. S. Rosseland, Astrophysik auf atomtheoretischer Grundlage. In *Struktur der Materie in Einzeldarstellungen* (Hrsg M. Born and J. Franck). Springer, Berlin (1931).
13. R. C. Weast, *CRC Handbook of Chemistry and Physics* (65th Edn 1984–1985), Tab. E-3. CRC Press, Boca Raton (1984).
14. H. Kuchling, *Taschenbuch der Physik*. Harri Deutsch, Thun and Frankfurt/Main 3, Auflage (1981).
15. Y. S. Touloukian, R. W. Powell, C. Y. Ho and P. G. Klemens, *Thermophysical Properties of Matter*, Vol. 2: *Thermal Conductivity—Nonmetallic Solids*. IFI/Plenum, New York/Washington, DC (1970).